Coincidence Detection of Photons

Ramish Ashraf
Roll no: 2017-10-0043
Supervised by: Dr. Sabieh Anwar
LUMS School of Science and Engineering

June 2, 2017

Contents

Acknowledgement

I would like to thank you Dr. Sabieh for allowing me to work with him on this project. His insight were invaluable and have helped me immensely. As a result of his constant probing, I feel like I have gained vital research skills that will help me in my future endeavors. I would also like to thank you Shafique Sb for helping with the fabrication and implementation of the circuit. Without him, the project would not have been completed on time.

Abstract

Coincidence counting modules(CCM) are a central part of experiments on quantum optics. However, the cost attached with a typical CCM renders them inaccessible for many undergraduate labs. A typical CCM would include Time-to-Amplitude Converters (TACS), a Nuclear-Instrumentation module (NIM) and a bin to house them. The costs add up to around 10000$. Our proposed design drastically lowers the cost by employing fast logical AND Gates. Moreover, by employing logical gates the effect of dead time can also be minimized.

1 Introduction

Coincidence detection is the simultaneous detection of two or more photons in different detectors. It is of cardinal importance in physics. Experiments related to coincidence detection are widely used in quantum optics. Coincidence detection can be used to detect a truly quantum light which will have a second order correlation function, $g^{(2)}(0) < 1$. Furthermore, coincidence detection also plays a vital role is the determination of lifetime of a muon; coincidence techniques are used to measure the time delay between the detection of μ^+ and e^+ particles [1]. A Time-to-Amplitude Converter (TAC) can then be used to convert the time delay in to a voltage. From this, the mean lifetime of a muon can be detected.

2 Theoretical background

2.1 Photon Statistics

The discussion in this section closely follows the book 'Quantum Optics: An Introduction' by Mark Fox [2].Suppose that a low beam light is incident on a detector. The basic function of the experiment is to count the number of photons that strike the detector in a user-specied time interval T. Quantum mechanically, the beam of light consists of a stream of photons. The photon flux φ is dened as the average number of photons passing through a cross-section of the beam in unit time. φ is easily calculated by dividing the energy flux by the energy of the individual photons:

$$\varphi = \frac{IA}{\hbar\omega} = \frac{P}{\hbar\omega} \text{ photons s}^{-1} \tag{1}$$

where A is the area of the beam and P is the power.

Photon-counting detectors are characterized by their quantum efficiency η, which is dened as the ratio of the number of photo-counts to the number of incident photons. The average number of counts registered by the detector in a counting time T is thus given by:

$$N(t) = \eta\varphi T = \frac{\eta P}{\hbar\omega} \text{ counts s}^{-1} \tag{2}$$

The maximum count rate that can be registered using a photon-counting system is usually limited by the dead-time effect. Dead-time effects stems from the fact that

every system needs a little time to reset once it has detected a photon. Dead-time is usually on the order of 1 μs which sets the upper limit on R of around 10^6 counts s^{-1}.

The photon flux given in equation 1 and 3 represent the average properties of the beam. A beam with a well-defined average will still show photon number fluctuations at short intervals. This is a consequence of the fact the light consists of photons which are inherently discreet. The fluctuations from the average are described by the **photon statistics** of the light.

2.2 Poissonian Photon Statistics

The most stable light one can think of is a perfectly coherent with a constant angular frequency ω, φ, and an amplitude A. The intensity of a beam of light is the amplitude squared and so there would be no intensity fluctuations since the amplitude is constant for a perfectly coherent light and the average photon flux would be constant. One would infer that a constant photon flux would consist of a stream of photons that are equally apart temporally. However, this is not the case. As mentioned above, there will be small fluctuations at small time scales. In fact, using rigorous mathematics one can show that the photon statistics for a coherent light wave with constant intensity is defined by **Poisson Distribution**

$$\rho(n) = \frac{\bar{n}}{n!} e^{-\bar{n}},\ n = 0, 1, 2 \ldots \tag{3}$$

Poissonian statistics generally apply to random processes. Randomness in a coherent light arises from the fact that there is an equal probability of finding a photon in a beam within any given time interval. Poisson distributions are characterized by their mean value $\bar{n}$ and the fluctuations of a statistical distribution about its mean value are usually quantified by the **variance**. The variance is also equal to the square of the **standard deviation**. For a Poissonian distribution the variance is equal to the mean value:

$$\Delta(n)^2 = \bar{n} \tag{4}$$

Where $\bar{n}$ is the mean value. Also standard deviation is given by the following expression:

$$\Delta n = \sqrt{\bar{n}} \tag{5}$$

2.3 Classification of Light through Photon Statistics

In the previous section we established that a perfectly coherent light has photons that are distributed randomly i.e Poisson distribution. Classically, a coherent light can be treated as the most stable light. So keeping this as a benchmark one can classify other types of light according to the standard deviation of their photon number distributions. There are three possibilities:

- sub-Poissonian statistics $\Delta n < \sqrt{\bar{n}}$
- Poissonian statistics $\Delta n = \sqrt{\bar{n}}$
- super-Poissonian statistics $\Delta n > \sqrt{\bar{n}}$

The difference between the three possibilities can visualized as shown below in Figure 1. The gure compares the photon number distributions of the three possibilities mentioned above with the same mean mean number of photons. We see that distributions of super-Poissonian and sub-Poissonian light are, respectively, broader or narrower than the Poisson distribution.

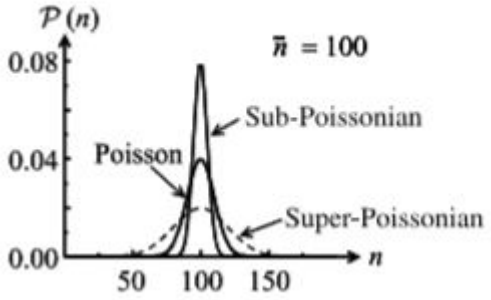

Figure 1: Taken from Mark Fox's Quantum Optics Fig 5.4 [2].

As we have already seen, coherent light results in a Poissonian distribution of photons. If there are any classical fluctuations, then one would expect large photon number distributions. Such a light would exhibit super-Poissonian statistics. This kind of light is commonplace e.g. light from a LED etc.

However, sub-Poissonian distribution has a narrower distribution than the Poissonian case. This would imply that there's a light that's more stable then a perfectly coherent light. This is non-intuitive, but not surprising since sub-Poissonian light comes under the domain of quantumn phenomena; it has no classical counterpart. Needless to say, observation of sub-Poissonian light is quite difficult but is a clear signature of the quantum nature of light.

2.4 Second-order correlation function

Hanbury Brown and Twiss while working on the intensity interferometer hypothesized that intensity fluctuations of a beam of light are related to its degree of coherence. It's now helpful to introduce the **second-order correlation function** of the light defined by:

$$g^{(2)}(t) = \frac{\langle I(t)I(t+\tau)\rangle}{\langle I(t)\rangle\langle I(t+\tau\rangle} \tag{6}$$

The $\langle ...\rangle$ symbols indicate the time average computed by integrating over a long time period. Consider, now, a light which has a constant intensity such that $\langle I(t)\rangle = \langle I(T+\tau)\rangle$. Also assume that the light is spatially coherent. In such circumstances the second-order correlation function investigates the *temporal* coherence of the source. Essentially, $(g^{(2)}(t))$ quantifies the intensity fluctuations. For times greater then the τ_c, the intensity fluctuations at times t and $t+\tau$ will be completely unrelated with each other:

$$I(t) = \langle I\rangle + \Delta I(t) \tag{7}$$

where $\Delta I(t)$ is the fluctuation from the mean value $\langle I\rangle$.

Moreover, $\langle \Delta I(t)\rangle = 0$

$$\begin{aligned}&\langle I(t)I(t+\tau)\rangle_{\tau\gg\tau_c} = \langle(\langle I\rangle + \Delta I(t))(\langle I\rangle + \Delta I(t+\tau)\rangle\\ &= \langle I\rangle^2 + \langle I\rangle\langle\Delta I(t)\rangle + \langle I\rangle\langle\Delta I(t+\tau)\rangle + \langle\Delta I(t)\Delta I(t+\tau)\rangle\\ &= \langle I\rangle^2\end{aligned}$$

Therefore, it's clear that:

$$g^{(2)}(\tau \gg \tau_c) = \frac{\langle I(t)I(t+\tau)\rangle}{\langle I(t)\rangle^2} = \frac{\langle I(t)\rangle^2}{\langle I(t)\rangle^2} = 1 \tag{8}$$

While on the other hand , if $\tau \gg \tau_c$ there will be some sort of correlation between the fluctuations at the two times. At $\tau = 0$,

$$g^{(2)}(0) = \frac{\langle I(t)^2\rangle}{\langle I(t)\rangle^2} \tag{9}$$

It can be shown that for any time dependence of $I(t)$:

$$g^{(2)}(0) \geq 1 \text{ and } g^{(2)}(0) \geq g^{(2)}(\tau) \tag{10}$$

These results can be explained intuitively. Consider a perfectly coherent monochromatic source with a time independent intensity I_o. In this case,

$$g^{(2)}(\tau) = \frac{\langle I(t)I(t+\tau)\rangle}{\langle I(t)\rangle^2} = \frac{{I_o}^2}{{I_o}^2} = 1 \tag{11}$$

for all values of τ since I_o is constant. Also, recall that (eq 8) that for large τ $g^{(2)}(\tau) = 1$. Finally consider any source with a time-varying intensity. It is apparent that $\langle I(t)^2\rangle > \langle I(t)\rangle^2$ because there are equal intensity fluctuations above and below the average, and the squaring process exaggerates the fluctuations above the mean value. So we must always have $g^{(2)}(0) > 1$. So essentially, for any source with a time-varying intensity, we expect $g^{(2)}(\tau)$ to decrease with τ, reaching unity for large values of τ. In the case for a coherent constant source, $g^{(2)}(\tau) = 1$ for all times.

Light source	Property	Comment
All classical light	$g^{(2)}(0) \geq 1$ $g^{(2)}(0) \geq g^{(2)}(\tau)$	$g^{(2)}(0) = 1$ when $I(t) =$ constant
Perfectly coherent light	$g^{(2)}(\tau) = 1$	Applies for all τ
Gaussian chaotic light	$g^{(2)}(\tau) = 1 + \exp\left[-\pi(\tau/\tau_c)^2\right]$	$\tau_c =$ coherence time
Lorentzian chaotic light	$g^{(2)}(\tau) = 1 + \exp\left(-2\lvert\tau\rvert/\tau_0\right)$	$\tau_0 =$ lifetime

Figure 2: Table taken from Mark Fox's Quantum Optics (Page 112, Table 6.1) [2].

2.5 Second Order Correlation Function in Terms of Photons

In the previous section the $g^{(2)}(\tau)$ function was classically discussed in terms of intensity correlations. Since the number of counts registered on a photon-counting detector is directly proportional to the intensity, we can write the expression in terms of the number of photons.

$$g^{(2)}(\tau) = \frac{\langle n_1(t) n_2(t+\tau)\rangle}{\langle n_1(t)\rangle \langle n_2(t+\tau)\rangle} \tag{12}$$

where $n_i(t)$ is the number of counts registered on detector i at time t. This shows that $g^2(\tau)$ is dependent on the simultaneous probability of counting photons at time t on detector 1(D1) and at time $t + \tau$ on detector 2(D2).

Completely different results are possible when one thinks of light in terms of photons as opposed to an electromagnetic wave. Suppose that light consists of a stream of photons with long time intervals in between them. Suppose now that this light is incident on a beam splitter with two detectors at the end.The photons that impinge on the beam splitter are randomly diverted to either D1 or D2. There is therefore a 50% probability that a given photon will be detected by either of the detectors. Suppose that a photon is detected by D1. Now there's no probability that a photon would detected at the same time by D2 since we initially assumed that photons are at long intervals apart. Hence, the timer will record no event at $\tau = 0$. We therefore have a situation where we expect no event at $\tau = 0$ but some events for larger values of τ; this clearly contradicts the classical result that was predicted earlier that $g^{(2)}(0) > 1$. We thus immediately see that the experiment with photons can give results that are not possible in classical theory of light. Remember that this result was only possible because we assumed that the input light consisted of individual photons with long time intervals in between. Now imagine a slightly different picture in which the photons are bunched together. Half of the photons are split towards D1 and the other half towards D2. These photons will strike the two detectors at the same time and there will be a high probability that both detectors register simultaneously. Therefore there will be large number of events near $\tau = 0$. As τ increases the number of events recorded drops. We thus have a situation with many events near $\tau = 0$ and fewer at later times, which is fully compatible with the classical results.

In conclusion, if one views light bin terms of photons, one can get results that are sometimes in line with the classical picture and at other times they give results that are completely opposite to what one would expect from the classical picture. The key difference here is the time interval between the photons; that is, whether the photons are regularly spread apart or come in bunches.

2.6 Photon Bunching and Antibunching

Earlier a threefold distinction was made depending on whether the photon statistics were sub-Poissonian, Poissonian or super-Poissonian. Now, another threefold classification will be made using the second order correlation function, $g^{(2)}(\tau)$. The classication is based on the value of $g^{(2)}(0)$ and proceeds as follows:

- Bunched Light $g^{(2)}(0) > 1$
- Coherent Light $g^{(2)}(0) = 1$
- Antibunched Light $g^{(2)}(0) < 1$

Bunched and Coherent light are in agreement with classical results. However, antibunched light is not. Antibunched light has not classical counterpart and is a truly quantum phenomena.

2.6.1 Bunched Light

For Bunched light, $g^{(2)}(0) > 1$. Evident from the name, such a light consists of a stream of photons with the photons all clumped together in bunches. This implies that if we detect a photon at time $t = 0$, there is a high probability of detecting another photon at short times than at long times. Therefore, we expect $g^{(2)}(\tau)$ to be larger for small values of τ than for longer ones, so that $g^{(2)}(0) > g^{(2)}(\infty)$. Bunched light is consistent with classical results. Chaotic light (incoherent) light from a discharge lamp is bunched. Since the number of photons is directly proportional to the instantaneous intensity, there will be more photons in the time intervals with high-intensity and fewer in the low-intensity intervals.The photon bunches will therefore coincide with the high-intensity time intervals.

2.6.2 Coherent Light

As we have seen earlier, a perfectly coherent light has Poissonian photon statistics, with random time intervals between the photons. The probability of obtaining pulses at the two detectors simultaneously remains constant for all values of τ. Therefore, a coherent light has $g^2(\tau) = 1$ for all values of τ.

2.6.3 Antibunched Light

In antibunched light the photons are equally spaced apart at large time intervals rather than being bunched together. If a photon is detected at D1, it's highly unlikely that another photon will be detected simultaneously at D2. Hence antibunched light has $g^{(2)}(0) < g^{(2)}(\tau)$ and $g^2(0) < 1$. This is in violation of classical results. Previously, we concluded that sub-Poissonian light, like antibunched light, is a clear indication of the quantum nature of light. Although the two phenomena are not identical, it will almost always be the case that non-classical light will exhibit both antibunching and sub-Poissonian photon statistics. Below is a schematic explanation of the three types of light studied above:

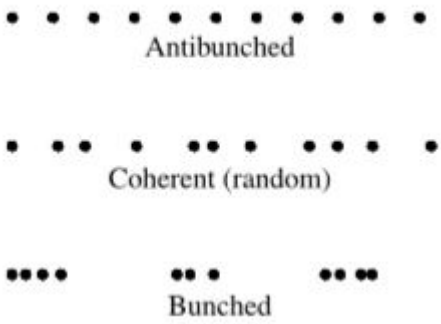

Figure 3: Comparison of the stream of photons of Antibunched, Bunched, Coherent Light[2].

3 Literature Review

We have seen how crucial a role the second order correlation function and coincidence counting of photons play in quantum optics. It is now imperative to mention certain techniques that have been used to demonstrate these phenomena.

One of the first experiments to demonstrate the existence of a non-classical eld was performed by Kimble, Dagenais, and Mandel in 1977 [3]. They measured the light emitted by a single atom and found $g^{(2)}(0) = 0.4 \leq 1$, proving that the field was antibunched. An antibunched field can be thought of as a field in which photons are not clumped together and arrive one at a time. Despite clearly demonstrating the phenomena of antibunched light, this experiment had its drawbacks. The experiment was complicated by the difficulty of isolating the light coming from the atom from the background scattered light.

A much more simpler demonstration of photon antibunching was performed by Grangier, Roger, and Aspect in 1986 [4]. A schematic of their experiment is show above. They avoided the problem of background light by using a two-photon cascade in Ca. Ca atom absorbs two photons from two lasers operating at frequencies f_{l1} and f_{l2}. As a result the atom is promoted to an excited state. The Ca atom then decays by emitting two photons at different frequencies: one at frequency f_1 by decaying to a intermediate level, and a second at frequency f_2 by decaying to the ground state. All four frequencies are distinct and can be isolated using filters. This reduces the problem of background scattering. The two photons are always emitted in opposite directions. The detection of one photon at one detector ensures that there would be a photon heading in the opposite direction, so that the first photon could be used as a gate to tag the arrival of the second. In this experiment, detections at T and R were conditioned upon detections at the gate detector (G). The measured degree of second order coherence/correlation is give in terms of probabilities by

$$g^{(2)}(0) = \frac{P_{GTR}}{P_{GT}P_{GR}} \tag{13}$$

Here P_{GT} and P_{GR} is the probability of detecting simultaneously a photon at detector T and R respectively and P_{GTR} is the probability of obtaining a threefold coincidence at detectors T,G and R. The probabilities can be written as

$$P_{GTR} = \frac{N_{GTR}}{N_G},\ P_{GT} = \frac{N_{GT}}{N_G},\ P_{GR} = \frac{N_{GR}}{N_G} \tag{14}$$

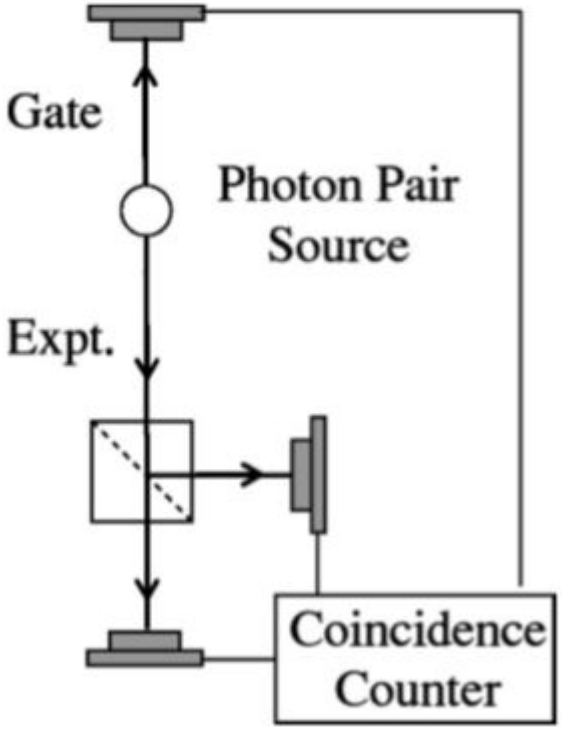

Figure 4: A source emits pairs of photons simultaneously that travel in opposite directions. Detection of the gate signal tells the T and R detectors when to expect a detection on the experiment side [4].

where, given a specied time window, N_{GT} and N_{GR} is the number of simultaneous detections at detector T,R and detector G and N_{GTR} is the number of threefold coincidences, and N_G is the number of singles counts at detector G. Plugging these expressions back into Equation 13 we get:

$$g^{(2)}(0) = \frac{N_{GTR}N_G}{N_{GT}N_{GR}} \tag{15}$$

Using this equipment, Grangier *et al.* measured a second order correlation of $g^{(2)}(0) = 0.18 \pm 0.006$. Advancement in technology has meant that the same experiment now measures $g^{(2)}(0)$ as 0.0188 ± 0.0067. However these calculations don't take into account the problem of accidental counts due to dead-time effects.

Another such series of experiment were performed by Mark Beck [5]. Two different experimental setups were designed for two fold and threefold coincidences. The schematics are shown in Figure 5 and 6

Beck defines two different second order correlation functions for each experiment. The threefold coincidence setup is similar in nature to the one Grangeir *et al.* designed. Infact, all the equations from 13 to 15 are perfectly valid for this setup. The only difference here is in the generation of photons. A down conversion crystal is now used instead of a Ca atom. The two-fold coincidence setup is also straight forward. Following a similar analysis used above one finds that the second order correlation function can be expressed in terms of probabilities but additionally one needs to specify a time

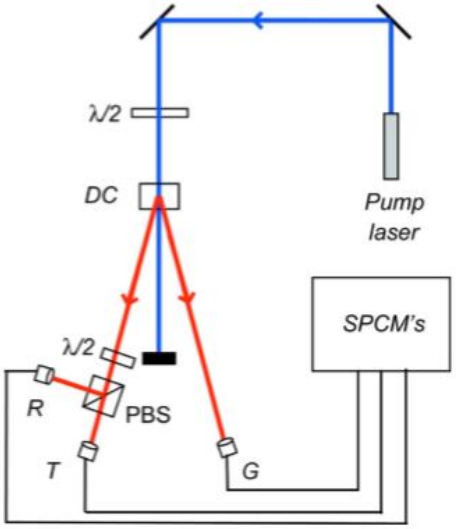

Figure 5: Three Fold Coincidence [5]

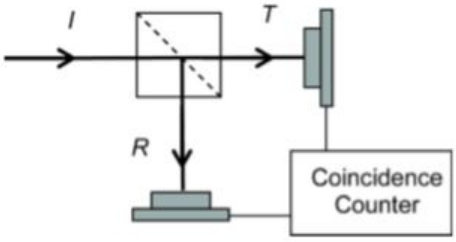

Figure 6: Two-Fold Coincidence Detection [5]

interval Δt and total counting time ΔT. The general expression is intuitive:

$$g^{(2)}_{2D}(0) = \frac{P_{TR}}{P_T P_R} \tag{16}$$

Here, Beck adds the subscript 2D to differentiate from the expression for the threefold coincidence. To experimentally measure the probabilities one makes use of the count rates and there is where the Δt and ΔT come in handy. For example, the probability of a detection at detector T within Δt is simply given by the average rate of detections at T, R_T, multiplied by Δt. The average rate is just the total number of detections N_T divided by the total counting time ΔT. The probabilities for R detections and TR coincidences are given similarly:

$$\begin{aligned} &P_T = R_T \Delta t = (\tfrac{N_T}{\Delta T})\Delta t, \;\; P_R = R_R \Delta t = (\tfrac{N_R}{\Delta T})\Delta t, \\ &P_{TR} = R_{TR}\Delta t = \tfrac{N_{TR}}{N_T N_R}(\tfrac{\Delta T}{\Delta t}) \end{aligned} \tag{17}$$

Substituting these equations in to Equation 16 results in:

$$g^{(2)}_{2D}(0) = \frac{N_{TR}}{N_T N_R}(\frac{\Delta T}{\Delta t}) \tag{18}$$

However, the above expressions still don't account for accidental counts due to dead time effects. Beck came up with a neat little algorithm to overcome this. However, before diving in to the algorithm, it's important to know what exactly is dead-time effect and how much role it plays in different coincidence measuring techniques. Dead time refers to the fact that once a photon is detected, certain instruments require time to reset. During this dead time further counts cannot be processed. This leads to missed coincidences and measurements of second-order correlation function are effected. Certain coincidence detection techniques which employs fast AND Gates to detect coincidences hardly suffer from any dead time [5].

Time-to-Amplitude Conversion (TAC) is a technique that has also been widely used in coincidence detection. However, TAC suffers greatly from dead time effects. The

dead time in the TACs frequently used to measure coincidences is on the order of 1 μs. For a periodic train of photons, it is possible to operate a TAC at rates approaching 10^6 counts per second (cps). However, if the photons are produced at random times, even if the average time between photons is more than 1 μs, there is some probability that photons are separated by less than this and coincidences will be missed. However, since TACs are so widely used in coincidence detection, it's essential we we talk about what exactly is a TAC and how is it generally implemented.

A TAC operates by receiving two inputs, called START and STOP, and then outputting a pulse, the amplitude of which is proportional to the time interval between the rising edges of the START and STOP signals. The proportionality between the amplitude and the time interval is controlled by the gain of the TAC. To ensure that the START pulse precedes the STOP pulse, an extra length of coaxial cable is usually inserted, corresponding to a delay of approximately 6 ns, between START and the STOP input. So if the there's simultaneous detection, the delay between START and STOP signals would 6 ns. A single channel analyzer (SCA) is also used in conjunction with a TAC. The SCA operates by receiving an input pulse, and then outputting a pulse with an amplitude of 5 V only if the amplitude of the input pulse falls within a certain voltage window. The width of the window is adjustable, as is the lower level of the window. The input to the SCA is the output from the TAC.

In order to measure the threefold GTR coincidences such as the one in Figure 5, T is used as the START input and R as the STOP input. To ensure that these TR coincidences also are coincident with a detection at G, the TAC is operated in start gate coincidence mode, and the G signal is input in to the START GATE input of the TAC. If an output pulse from G is not present at the START GATE when the pulse from T arrives at START, then the timing circuitry in the TAC is disabled, and no output is produced. A simple TAC is usually implemented using transistors. One such implementation is show below:

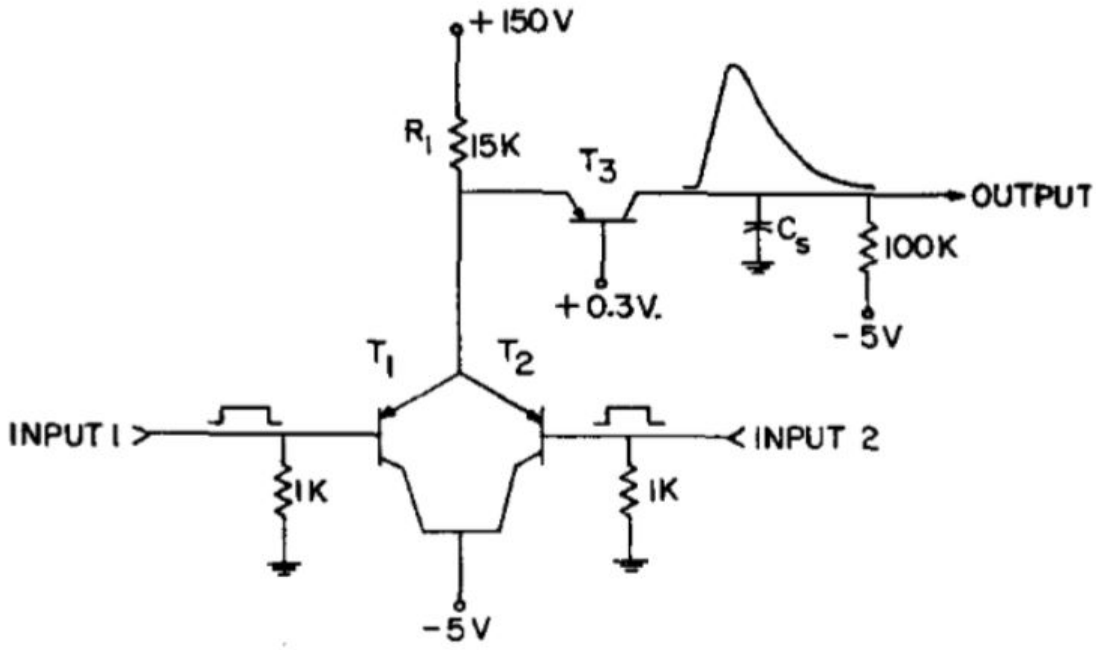

Figure 7: Simplified View of a TAC [6]

A simplified diagram of the time-to-amplitude converter is shown in Figure 7. Initially,

the two input transistors T_1 and T_2 are conducting, and the output transistor T_3 is cut off. The resistor R_1 serves as a constant current source. When one of the input transistors is cutoff by a positive pulse, all of the current I flowing through R_1 is carried by the other input transistor and T_3 remains cut off. When a coincidence occurs, both T_1 and T_2 are cut off, and the current I is switched into T_3. This current is integrated at the collector of T_3, therefore the amplitude of the output pulse is given by $V = \frac{I\Delta t}{C}$. C is the stray capacitance at the collector of T_3, and Δt is the period of time that both T_1 and T_2 are cut off. As long as I and C are constant, V is directly proportional to the time overlap of the two input pulses.

Coming back to the problem of dead-time effects and missed coincidences , it was stated earlier that circuits that employ TAC to detect coincidences suffer from dead-time effects. However, it was also mentioned that M.Beck used an neat little algorithm which can overcome these dead-time effects. The algorithm is now discussed in detail.

Each TAC has an output labeled VALID START (VS). Every time a START pulse successfully initiates a conversion event, there is a VS output pulse. Suppose that one START pulse initiates a conversion event; for this conversion event the TAC outputs a VS. If a second START pulse arrives within the dead time, it cannot initiate a conversion event, and hence no VS pulse is output. Since this second START pulse does not initiate a conversion event, it cannot contribute to the measured coincidences. This is what leads to missed coincidences using TACs. However, there is a way to correct the measurements. The key to doing this is to realize that when measuring $g^{(2)}(0)$, only START pulses that trigger a VS can possibly contribute to a measured coincidence.

Consider first, the two-fold coincidence circuit shown in Figure 6. The T detector serves as the START pulse. Only detections at T which trigger a VS will contribute to the coincidence measurements. The normalization in equation 18 is then erroneous. One needs to normalize by $N_{T_{VS}}$ and not N_T. The equation now becomes:

$$g^{(2)}_{2D}(0) = \frac{N_{TR}}{N_{T_{VS}} N_R} (\frac{\Delta T}{\Delta t}) \tag{19}$$

Notice that, N_R is not replaced by $N_{R_{VS}}$ because the R detector is connected to the stop input of the TAC.

Now consider the three-fold coincidence setup in Figure 5. Since three coincidences are needed, we need three TACs. The denominators used to calculate the probabilities in equation 14 will be replaced by the corresponding number of VSs. The correct expressions now are:

$$P_{GT} = \frac{N_{GT}}{N_{G_{VS}}}, P_{GR} = \frac{N_{GR}}{N_{G_{VS}}} \tag{20}$$

Notice that the expression for threefold coincidence hasn't been modified. This is because the experiment is setup in such a way that dead time has no effect on three fold coincidences. Taking all of this into account the expression for the second-order correlation function becomes:

$$g^{(2)}(0) = \frac{(N_{G_{VS}})^2 N_{GTR}}{N_G N_{GT} N_{GR}}$$

The values of $g^{(2)}(0)$ calculated from these values were almost similar to the circuits

which used fast logical AND gates. This shows that the algorithm proposed by M.Beck does indeed correct for missed coincidences due to dead-time effects.

In conclusion, one should aim to employ fast logical gates for coincidence counting purposes since they usually don't suffer dead-time effects (at least not as much as circuit which employs a TAC). However, one can account for missed coincidences and dead-time effects even when a TAC is used. This concludes the literature review.

4 Methodology

Having reviewed the literature, it's now time to go in to details of the methodology that we employed. The paper by D. Branning [7] was closely followed. The circuit makes use of fast logical AND gates and inverters. We have already seen that fast logic gates don't suffer from dead-time effects. Hence, there should be less missed coincidences as compared to a circuit which employs time-to-amplitude converters (TACs).

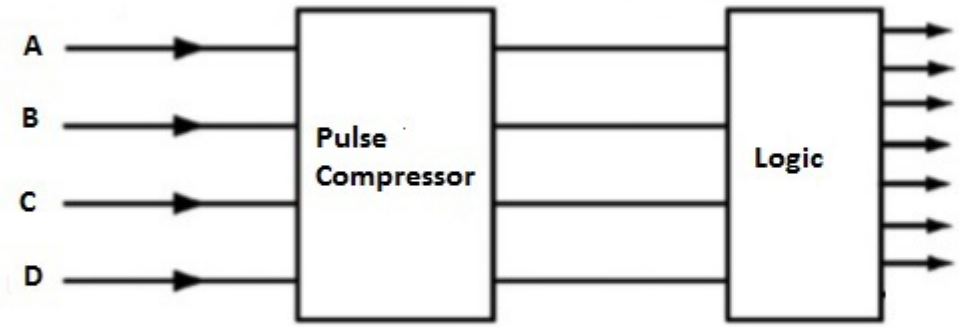

Figure 8: Block Diagram of the CCM Circuit.

In layman terms, the circuit works according to the following methodology: The pulses from the detectors are sent to the inputs of an AND gate, and the output of the gate is logically true (high) if and only if both inputs are simultaneously highthat is, if both detector pulses arrive at the gate at the same time.The design uses discrete F-series logic chips, which have a rise time of around $2 - 5\,ns$.

The input signals can be from a single photon counting module (SPCM) or any other detector. The pulses enter a pulse compressing circuit which either lets the signal pass through unchanged or changes the width of the pulse according to the setting of the 4 to 1 MUX. Reducing the pulse duration reduces the allowed time for two signals to overlap at the AND gates and reduces the number of accidental coincidences due to uncorrelated photons. The shortened pulses are passed to a logic section where AND gates are used to examine the various coincidence combinations selected by the user. Figure 8 shows a detailed circuit diagram of the pulse compressor for a single channel.

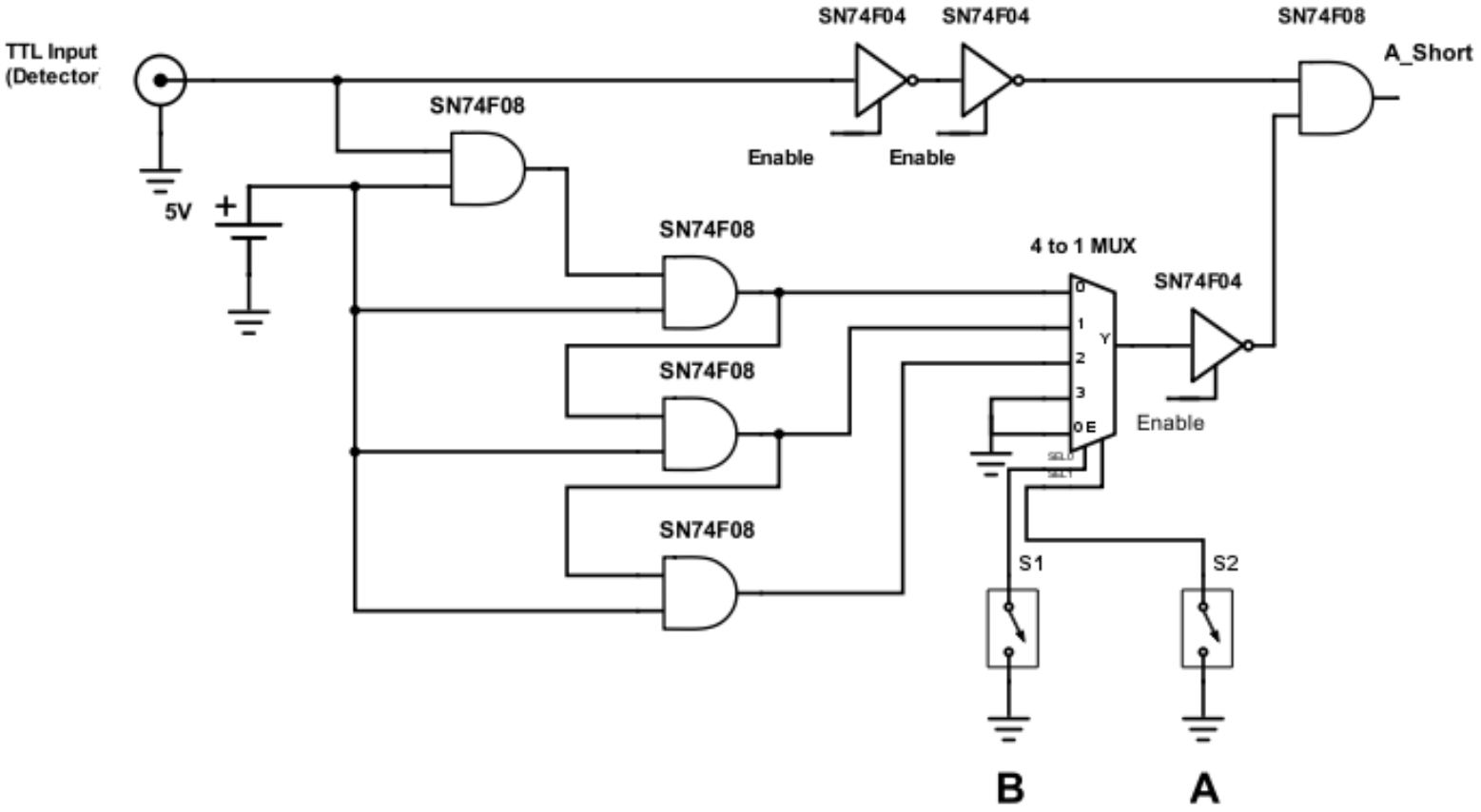

Figure 9: Schematic diagram of the pulse-compressing circuit.

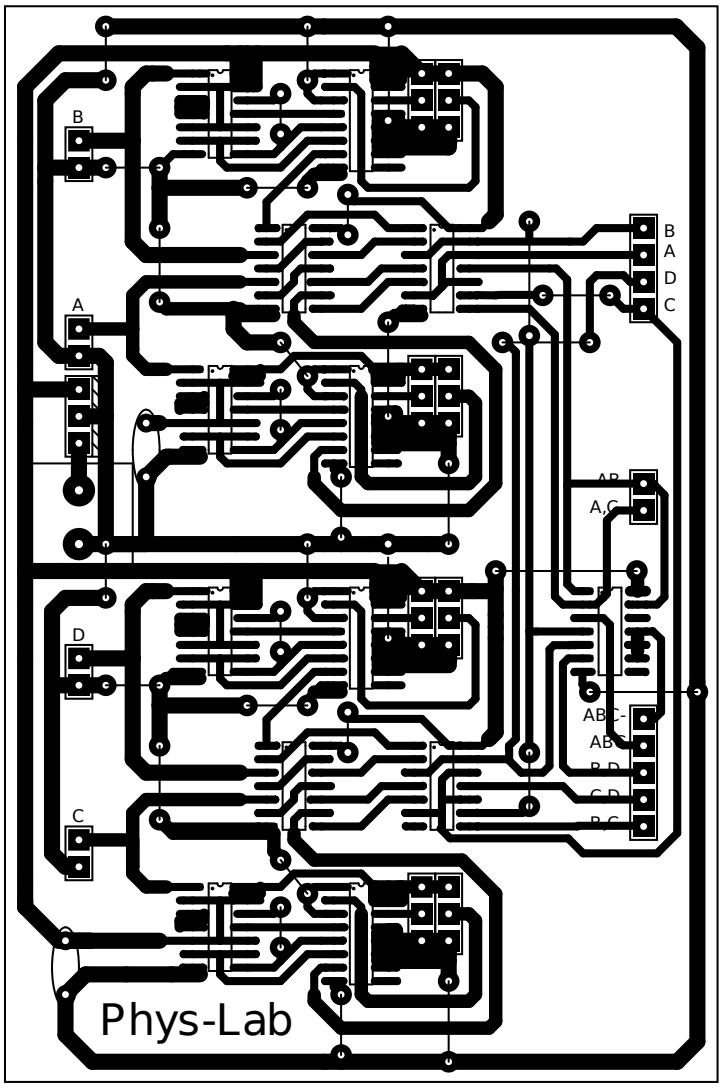

Figure 10: Blue Print of the whole circuit (Logic Unit + Pulse Compressor).

Table 1: Statistical data of the different widths obtainable. The average value and standard deviation were obtained from a data of 10 trials.

Channel	**00** (ns)	**01** (ns)	**10** (ns)	**11** (ns)
A	10.1 ± 0.2	12.8 ± 0.2	14.4 ± 0.2	58.9 ± 0.2
B	10.8 ± 0.1	13.0 ± 0.1	13.7 ± 0.2	60.5 ± 0.2
C	9.5 ± 0.1	12.2 ± 0.4	13.8 ± 0.1	58.9 ± 0.1
D	10.8 ± 0.3	13.1 ± 0.2	14.4 ± 0.1	59.6 ± 0.2
$A^{'}$	10.5 ± 2.7	13.0 ± 2.6	14.5 ± 0.2	63.7 ± 0.1
$B^{'}$	9.8 ± 1.2	12.3 ± 2.0	14.2 ± 0.2	65.1 ± 0.2
$C^{'}$	10.3 ± 1.0	12.5 ± 1.0	13.8 ± 0.4	63.7 ± 0.2
$D^{'}$	11.3 ± 0.8	13.1 ± 0.5	14.7 ± 0.5	64.4 ± 0.1

Pulse compressing is accomplished by using two copies of the same input signal. One copy is time-delayed and inverted with respect to the other copy. Both copies are then input in to an AND gate. The output of the AND gate will only be high for the duration of the time delay. The time delays are accomplished by sending the signal through additional gates, e.g., AND gates, that add delay to the signal. By changing the values of the two select lines, A and B, to either 1 or 0, different pulse widths can be obtained. The pulse compressing circuit can also be bypassed and the original pulse width would then be passed on to the logic section. The different widths that were obtained using this methodology are tabulated below. The widths were defined as full width at half maximum (FWHM).The data was obtained at a frequency of 100 KHz and the input signal pulse width was $60\,ns$. The widths were noted at different frequencies and pulse widths too but the results turned out to be the same i.e the pulse compressor compresses each signal to the same degree regardless of the initial pulse width and frequency. Instead of using SPCM's or detectors, we used a pulse generator, Rigol DG1022. The same input was given to all channels. It's imperative to mention that the type of connectors used in this setup is crucial. Since the pulses tend to be very close apart in time (i.e high frequency), the usage of cables that can not handle such high frequencies can give erroneous results. We used standard cables that come with a oscilloscope. Our CCM also includes inverted version of all the input signals. The different pulse widths, for each channel, were analyzed using a digital oscilloscope on a PC. One such set of graphs, for a single channel (A), is shown in Figure 10. Channels for other graphs were also similar in shape and were indistinguishable to the naked eye. However, to properly quantify these differences one can refer to the Table 1.

The logic section has seven output channels, which can register various two or threefold coincidence counts between combinations of input signals. The logic section simply employs AND gates. The output can only be high when there's an overlap between the two pulses or in other terms, the output will be high only at the instance when two photons strike simultaneously on to the two detectors. 7 different coincidences were implemented:

- AB
- AC
- BC
- BD
- CD
- ABC
- ABC'

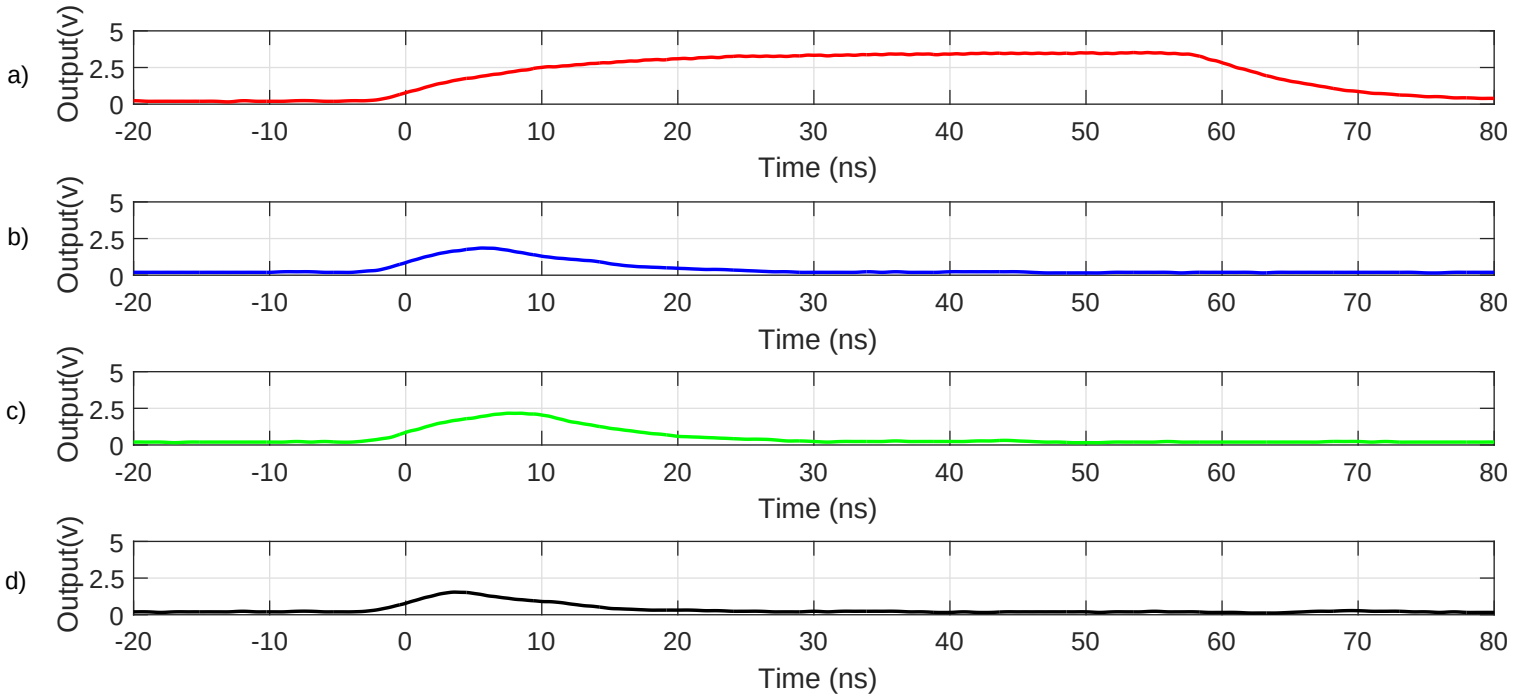

Figure 11: Pulse Widths for different settings on the MUX; a,b,c and d correspond to the select line setting of 11, 10, 01, 00 respectively. The graphs shown here are for Channel A. All other channels had pulses of similar width and shape.

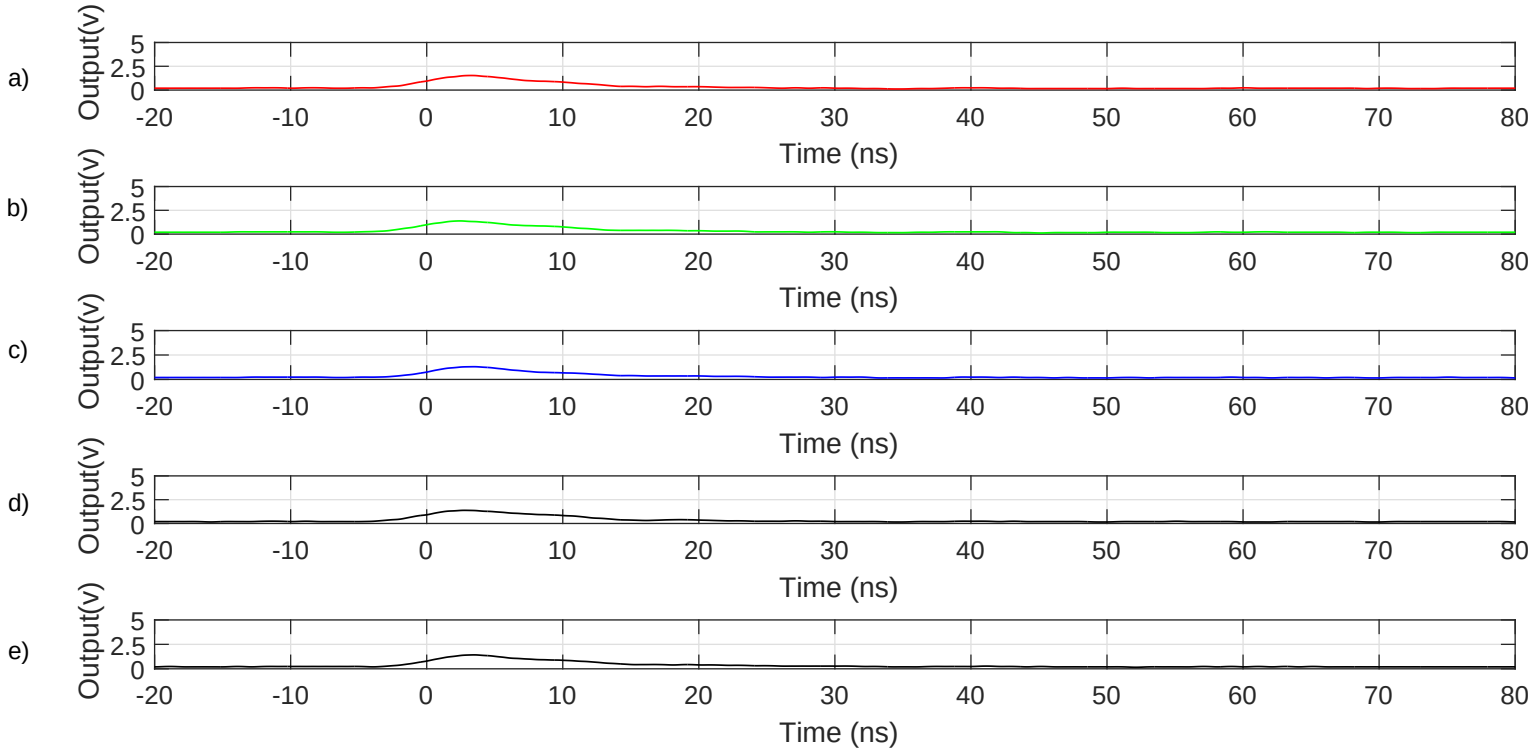

Figure 12: Two Fold Coincidences. a), b),c),d) and e) correspond to coincidences AB, AC, BC, BD and CD

Figure 12 shows two-fold coincidences. Inputs to each channel were provided from one of the channels of the pulse generator. 2 to 1 connectors were used at the output of the pulse generator so that the same pulse is input in to every channel on the CCM board. The select lines on the MUX were kept at 00 for each channel (i.e the shortest possible width). Since our circuit would only be high when both of the pulses are high, it is no surprise that output of this experiment also resulted in a width of approximately 10 ns. This is because the both of pulses were identical in shape and width. Figure 13 represents three fold coincidences. The output ABC will only be high when all input pulses are high. The second graph was obtained when the input to the channel C was disconnected. Since the graphs corresponds to $AB\bar{C}$, one would need no input at C to obtain an output. A trial was also performed with all inputs A, B and C high; this resulted in no output at the the $AB\bar{C}$ output.

A PCB was fabricated of the whole circuit (CCM + Logic). The PCB was then put inside a blackbox. The box had BNC connections for inputs at its back and at the front it had BNC connections for modified pulses and the coincidences. The black box is shown in the Figure 14 and the circuit blue print is shown in Figure 10. The list of equipment and their specifications are shown in the Table 2.

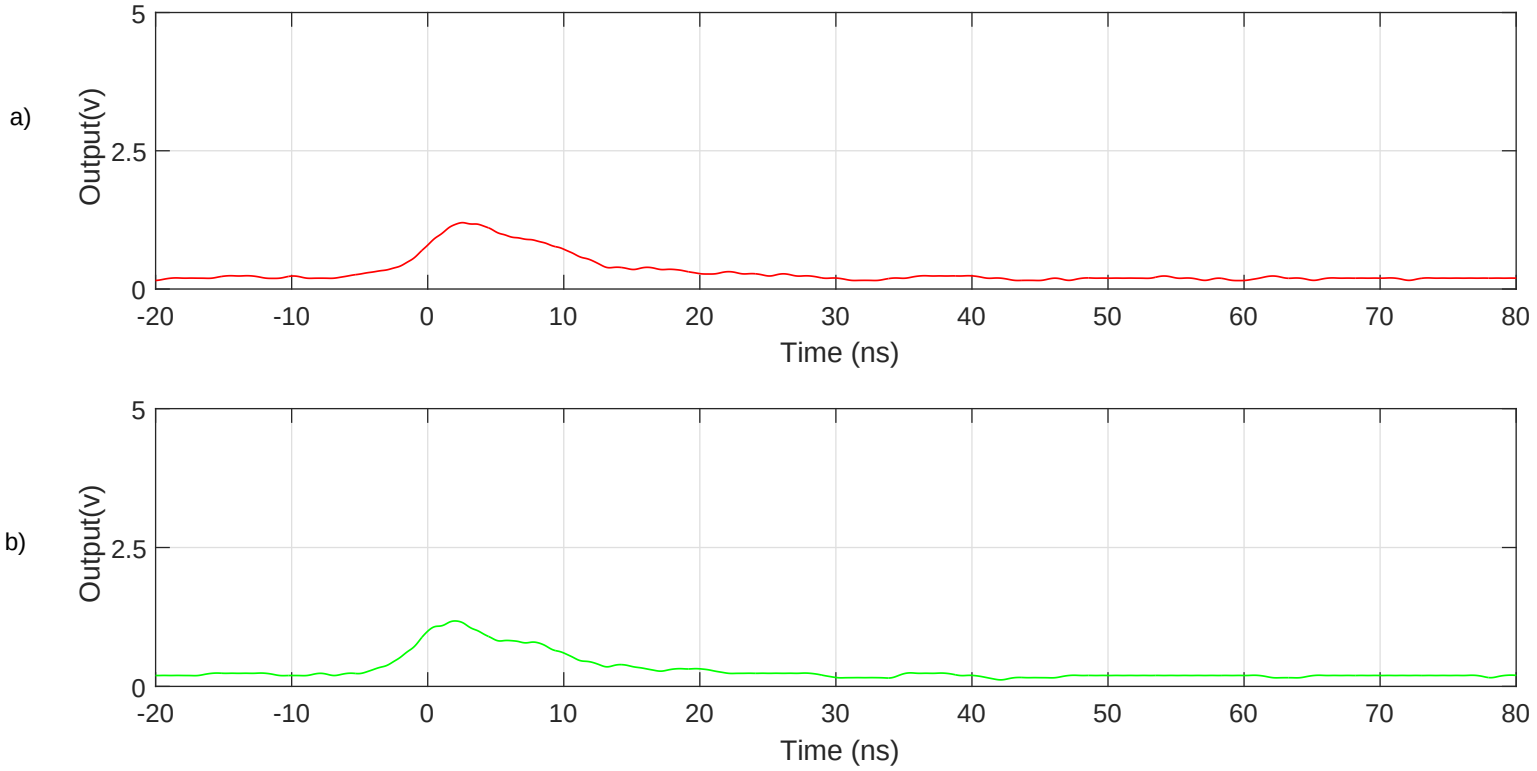

Figure 13: Two Fold Coincidences. a) and b) correspond to threefold-coincidences ABC and ABC'

(a) Front View.

(b) Back View.

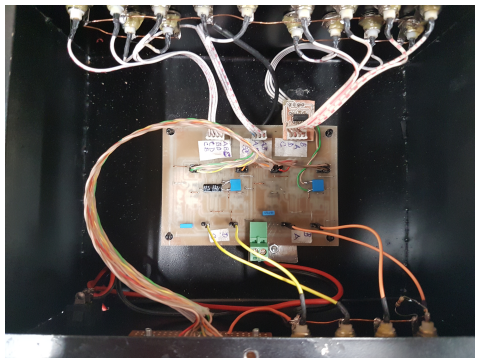

(c) Top View.

Figure 14: Different Views of the Black Box.

Component	Specifications
AND Gate (SN74F08)	Max Propogation Delay: 5 ns Logic Level- Low: 0.8 V Logic Level- High: 2.0 V Rise Time: 2-6 ns
Hex Inverter (SN74F04)	Max Propogation Delay: 5 ns Logic Level- Low: 0.8 V Logic Level- High: 2.0 V Rise Time: 1.6-6 ns
4 to 1 Multiplexer (SN74F153)	Logic Level- Low: 0.8 V Logic Level- High: 2.0 V Rise Time: 2-8ns
PicoScope 3000	2 Channels, BNC single-ended Bandwidth (∼3dB): 70Mhz Rise Time: 5.0ns Vertical resolution: 8 bits Maximum Sampling Rate: 10 MS/s
Pulse Generator (Rigol DG1022)	Frequency Range Pulse: 500 Hz - 3 MHz Resolution:1 Hz Channel 1: 5 V (50) 10 V (high impedance) Channel 2: ± 1.5 V (50) ±3 V (high impedance) Sample Rate: 100 MS/s

Table 2: Specifications of the equipment used.

References

[1] T. Sleator, D. Windt and B.Budick, "*The Muon Lifetime*", Experimental Physics V85.0112/G85.2075 (2005).

[2] M.Fox, "*Quantum Optics. An Introduction*", Oxford University Press, Ch5-6, (2006).

[3] H. J. Kimble, M. Dagenais, and L. Mandel, "*Photon antibunching in resonance uorescence*", Phys. Rev. Lett. 39, 691695 (1977).

[4] Grangier, G. Roger, and A. Aspect, "*Experimental evidence for a photon anti-correlation effect on a beam splitter: A new light on single-photon interferences*", Europhys. Lett. 1, 173179 (1986).

[5] M. Beck, "*Comparing measurements of* $g^2(0)$ *performed with different coincidence detection techniques*", J. Opt. Soc. Am. B 24, 2972-2978 (2007).

[6] P.C.Simms,"*Fast Coincidence System Based on a Transistorized Time-to-Amplitude Converter*", The Review of Scientific Instruments Vol 32, Num 8, (1961).

[7] D.Branning, S.Bhandari, M.Beck, "*Low-cost coincidence-counting electronics for undergraduate quantum optics*",American Journal of Physics 77, 667 (2009).